Adaptation of the binding domain of *Lactobacillus acidophilus* S-layer protein as a molecular tag for affinity chromatography development.

Emanuel J. Muruaga[1,2], Paula J. Uriza[1,2], Gonzalo A. K. Eckert[1,2], María V. Pepe[1,2], Cecilia M. Duarte[1,2], Mara S. Roset[1,2] * and Gabriel Briones[1,2] *.

1. Instituto de Investigaciones Biotecnológicas, Universidad Nacional de San Martín (UNSAM)- Consejo Nacional de Investigaciones Científicas y Técnicas (CONICET). 2. Escuela de Bio y Nanotecnologías (EByN), Universidad Nacional de San Martín.

Running title: The $SLAP_{TAG}$ affinity chromatography (SAC)

Keywords: Protein purification- Affinity chromatography- The $SLAP_{TAG}$.

*Corresponding author

Mailing address: Instituto de Investigaciones Biotecnológicas, Universidad Nacional de San Martín (IIB-UNSAM), Av. 25 de Mayo y Francia, Campus Migueletes, CP1650, San Martín, Buenos Aires, Argentina. Tel.: +54 11 4006-1500 (Int 2139); Fax: + 54 11 (5411) 4006-1559.

E-mail: gbriones@iib.unsam.edu.ar, mroset@iib.unsam.edu.ar

Abstract

The $SLAP_{TAG}$ is a novel molecular TAG derived from a protein domain present in the sequence of *Lactobacillus acidophilus* SlpA ($SlpA^{284-444}$). Proteins from different biological sources, with different molecular weights or biochemical functions, can be fused in frame to the $SLAP_{TAG}$ and efficiently purified by the specific binding to a bacterial-derived chromatographic matrix named here Bio-Matrix (BM). Different binding and elution conditions were evaluated to set an optimized protocol for the $SLAP_{TAG}$-based affinity chromatography (SAC). The binding equilibrium between $SLAP_{TAG}$ and BM was reached after a few minutes at 4°C, being the apparent dissociation constant (K_D) of 4.3 µM, a value which is similar to different Kd determined for other S-layer proteins and their respective bacterial cell walls. A reporter protein was generated (H_6-GFP-$SLAP_{TAG}$) to compare the efficiency of the SAC against a commercial system based on a Ni^{2+}-charged agarose matrix, observing no differences in the H_6-GFP-$SLAP_{TAG}$ purification performance. The stability and reusability of the BM were evaluated, and it was determined that the matrix was stable for more than a year, being possible to reuse it five times without a significant loss in the efficiency for protein purification. Alternatively, we explored the recovery of bound SLAP-tagged proteins by proteolysis using the $SLAP_{ASE}$ (a SLAP-tagged version of the HRV-3c protease) that released a tag-less GFP ($SLAP_{TAG}$-less). Additionally, iron nanoparticles were linked to the BM and the resulting BM_{mag} was successfully adapted for a magnetic SAC, a technique that can be potentially applied for high-throughput-out protein production and purification.

42 **Introduction**

43 Proteins are biopolymers formed by a particular amino acid sequence that determines a given atomic
44 spatial distribution, also known as protein conformation. Far from being a static structure, proteins behave
45 as nano-machines performing precise molecular activities due to internal movements of the protein parts
46 or protein domains [1]. In addition, proteins can interact intramolecularly or intermolecularly with different
47 macromolecules such as proteins, DNA, RNA, polysaccharides, or small compounds [2].

48 Proteins perform vital functions in life. For instance, some proteins degrade aliments to produce essential
49 nutrients (like digestive enzymes), others transport critical compounds for supporting life (like hemoglobin
50 that transports oxygen to the cells), or shape the cellular structure (like actin, tubulin, or keratin), or
51 function as hormones (like insulin), or defense the organism against pathogens (like the antibodies) [2].

52 In addition to the multiplicity of existent polypeptides in nature, molecular biology and biotechnology have
53 generated a myriad of chimeric proteins by combining different protein domains [3]. These artificial proteins
54 can be used as therapeutic tools to treat cancer, autoimmunity, or different medical conditions [4].

55 However, to gain value in therapy, in biochemical, industrial, or medical applications proteins require a
56 highly purified, stable, and concentrated state. This state is reached by a series of steps in the process of
57 separating the desired protein from the rest of all other proteins of a sample, free of contaminants, and
58 preserving its biological activity. The purification process exploits differences in size, charge,
59 hydrophobicity, ligand binding affinity, or specific sequences[5 6 7]. Several fractionations o chromatographic
60 steps can be combined for an efficient enrichment or purification of a particular protein.

61 Affinity chromatography is a special type of liquid chromatography that exploits the existence of natural [8]
62 or artificial [9] affinities between two moieties: the molecular target (or tag) and its ligand (the affinity ligand)
63 which is usually immobilized onto a chromatographic stationary phase to generate a chromatography
64 matrix. Thus, proteins of interest can be fused in-frame to different molecular tags (such as His-6X, GST,
65 MBP, etc.) expressed and purified ideally in a single step from a complex mixture of proteins.

66 Since it was developed by Starkestein in 1910 [10], affinity chromatography was gaining popularity and
67 centrality for many industrial processes such as the purification of proteins for diagnosis, research, and
68 therapeutic purposes [11]. Regulatory requirements for the purity and quality of the proteins vary greatly
69 depending on the area of application. For instance, bio-products can be used with little purification for
70 industrial use. Also, the recombinant protein produced for research, diagnosis, or non-clinical purposes has
71 a less stringent regulatory approval process than proteins designed as biopharmaceuticals.

72 The most common strategy for affinity chromatography is the ON/OFF format. In the "ON" phase, a
73 biological sample containing the protein of interest (that can be fused-in-frame to a molecular tag) is
74 formulated in a specific application buffer that will favor the binding process to a ligand. Then, the sample
75 is placed in contact with a chromatography material (or chromatography matrix) that has associated the
76 affinity ligand that consequently will recognize and retains the tagged protein. After the washes in the "OFF"
77 phase, an elution buffer is passed or incubated to release the tagged protein by changing the pH, the ionic
78 strength that modifies the affinity of the interaction (non-specific elution) or the addition of the free ligand
79 that will out-compete the retained tagged protein (bio-specific elution)[11].

80 The simplicity and specificity of affinity chromatography have made this technique central for the
81 purification of biomolecules and biopharmaceuticals.

82 Here, we explored the adaptation of a protein domain present in the carboxy terminus of the *Lactobacillus*
83 *acidophilus* protein SlpA as a molecular tag. *In silico* analysis of this region ($SlpA^{284-444}$) allowed us to identify
84 a tandem of two copies of the 60-aminoacid protein domain named SLP-A (pfam03217) which is necessary
85 for the association (Fig. Supp. 1). Here, this dual SLP-A domain was named $SLAP_{TAG,}$ and the adaptation as a
86 molecular tag was evaluated. Recently, we have characterized the binding properties of the $SLAP_{TAG}$ and
87 characterized its association with the cell wall of live *Lactobacillus* for vaccine purposes [12]. Thus, the $SLAP_{TAG}$
88 was fused in frame to a chimeric antigen derived from the Shiga toxin-producing *Escherichia coli* (STEC)
89 formed by the peptides $EspA^{36–192}$, $Intimin^{653–953}$ and $Tir^{240–378}$ (or EIT). The resulting chimeric antigen (EIT-
90 $SLAP_{TAG}$) recombinantly expressed and purified was able to associate with the bacterial cell wall of *L.*

91 *acidophilus*, a process that we named decoration. Thus, EIT-decorated *L. acidophilus* after oral
92 administration was able to deliver the EIT antigen to the intestinal mucosa eliciting a protective immune
93 response that controls an experimental STEC infection in mice [12]. Remarkably, the decoration process does
94 not modify genetically the *Lactobacillus* genome preserving its GRAS (Generally Recognized as Safe) status,
95 a trait that is important for vaccine purposes.

96 Here, we explore the adaptation of the $SLAP_{TAG}$ for the development of novel affinity chromatography, the
97 SLAP affinity chromatography (SAC), and a comprehensive protocol is presented.

98 **Results**

99 **SLAP$_{TAG}$ binds rapidly and efficiently to the Bio-matrix (BM)**

100 As described in the Methods section the SLAP$_{TAG}$ (Fig. Supp.1) was fused in-frame to the carboxy-terminus
101 of the green fluorescent protein (GFP) to generate the chimeric protein (H_6)-GFP-SLAP$_{TAG}$ adapted here as
102 a SLAP$_{TAG}$ reporter protein. As shown in Fig. 1A the structure of the chimeric protein (H_6)-GFP-SLAP$_{TAG}$ was
103 predicted based on the alphaFold-2 method [13]. The beta-barrel corresponding to GFP and the two globular
104 domains corresponding to SLAP$_{TAG}$ were predicted with high performance and as expected, linkers and
105 6xHis-tag, which are flexible regions, showed low prediction values.

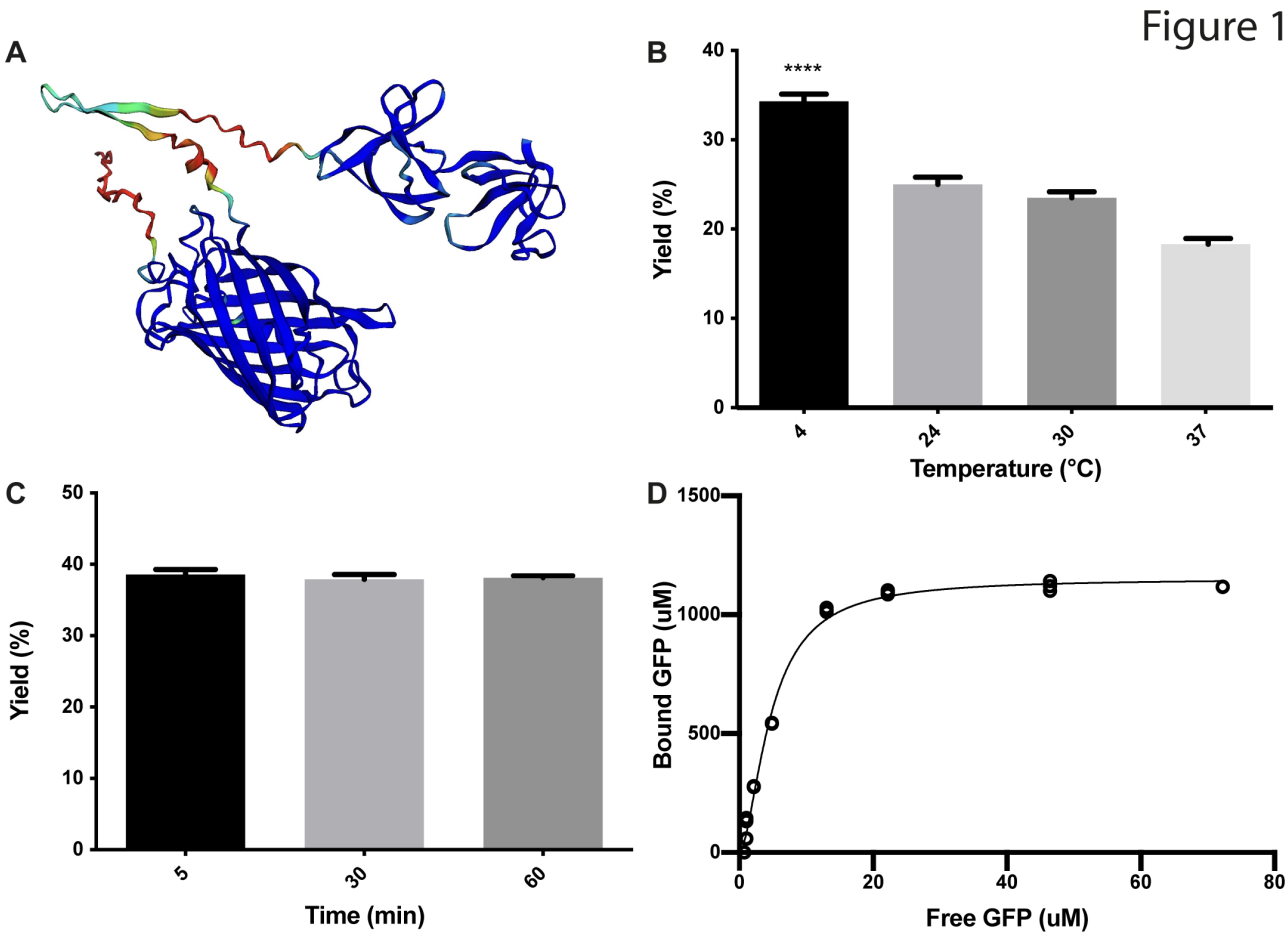

106

107 As a working chromatographic matrix, a culture of *Bacillus subtilis* natto was processed as described in the
108 Methods section to generate a bacterial-derived affinity chromatography matrix, named here Bio-Matrix
109 (BM). Interestingly, although *B. subtilis* has no S-layer, we have demonstrated previously that this bacterium
110 can be externally covered with SLAP-tagged proteins to generate a recombinant S-layer on its bacterial cell

111 wall, a process that we called decoration [12]. Decoration of *B. subtilis* with SLAP-tagged proteins is possible
112 because teichoic acid and lipoteichoic acid (which are the molecules responsible for the $SLAP_{TAG}$ association)
113 have the same chemical composition as *Lactobacillus acidophilus*. Interestingly, in *B. subtilis* and *L.*
114 *acidophilus,* teichoic acid and lipoteichoic acid are distributed homogeneously on their cell wall.

115 To characterize the binding properties of the $SLAP_{TAG}$, the reporter protein (H_6)-GFP-$SLAP_{TAG}$, was
116 recombinantly expressed in *Escherichia coli*, purified by affinity chromatography mediated by its Hisx6 tag
117 (H_6), and further incubated with BM under a variety of conditions. Initially, as shown in Fig. 1B, the optimal
118 binding temperature of (H_6)-GFP-$SLAP_{TAG}$ to the BM was evaluated, finding that the best binding efficiency
119 was reached when the incubation was performed at 4ºC. To get insights into the $SLAP_{TAG}$ association
120 dynamics, (H_6)-GFP-$SLAP_{TAG}$ was incubated for 5, 30, and 60 minutes with BM, and as shown in Fig. 1C, the
121 maximal binding of (H_6)-GFP-$SLAP_{TAG}$ to BM was reached very rapidly (already at 5 minutes), showing no
122 significant increments in its association at longer time points. These results indicated that the $SLAP_{TAG}$ binds
123 very rapidly and with an apparent high affinity to the BM. To quantify the affinity of the interaction between
124 the $SLAP_{TAG}$ with the BM, an adsorption isotherm was performed to determine the apparent equilibrium
125 dissociation constant as described in the Methods section. As shown in Fig. 1D the apparent K_D was
126 estimated as 4.7 µM. Interestingly, this dissociation constant value was in the same order as other K_D
127 described for different microbial S-layer proteins with their respective bacterial cell walls [14–16]. In addition,
128 the maximum adsorption capacity (Bmax) of BM was estimated as 1.152 mmol of (H_6)-GFP-$SLAP_{TAG}$ or 53.9
129 mg of protein per milliliter of BM or 1.03 g of $SLAP_{TAG}$ protein/g of dry BM.

130 **Elution of (H_6)-GFP-$SLAP_{TAG}$ protein can be performed with different buffers.**

131 As it was mentioned, the $SLAP_{TAG}$ contains the protein region responsible for the association of the protein
132 SlpA to the *L. acidophilus* cell wall. As reported, *L. acidophilus* SlpA has the natural ability to self-assemble
133 on the bacterial surface to generate a proteinaceous layer named S-layer [17], a highly ordered wall structure
134 that functions as a protective barrier against bacteriophages, resistance to low pH and proteases, and
135 bacterial adhesion. It is well characterized that removal of the S-layer can be performed efficiently by the

136 addition of chaotropic agents like LiCl, a compound that disrupts hydrogen bonds leading to a partial
137 denaturation of proteins and the consequent detachment of the S-layer [17]. To study (H_6)-GFP-SLAP$_{TAG}$
138 elution, LiCl solution was selected as the positive control. As shown in Fig. 2A while PBS (137 mM NaCl, 2.7
139 mM KCl, 8 mM Na2HPO4, and 2 mM KH2PO4) does not affect elution, the detachment of BM-associated
140 (H_6)-GFP-SLAP$_{TAG}$ was achieved with high efficiency with a 2M LiCl solution at room temperature, in a short
141 lapse of five minutes (Fig. 2B). As it was mentioned above, lithium solutions have deleterious effects on
142 proteins, which is an undesired effect for protein purification, especially for enzyme purification. Therefore,
143 different milder alternatives of buffers were explored to elute SLAP$_{TAG}$-tagged proteins, conditions that can
144 preserve the protein structure and therefore their function. As shown in Fig. 2C, a series of sugars
145 (monosaccharide and disaccharides) described previously [18] were tested for the elution of the reporter SLAP
146 observing a partial elution efficiency when compared with the LiCl elution control (Fig. 2C). Next, the
147 cationic nature of the SLAP$_{TAG}$ at neutral pH was considered.

148

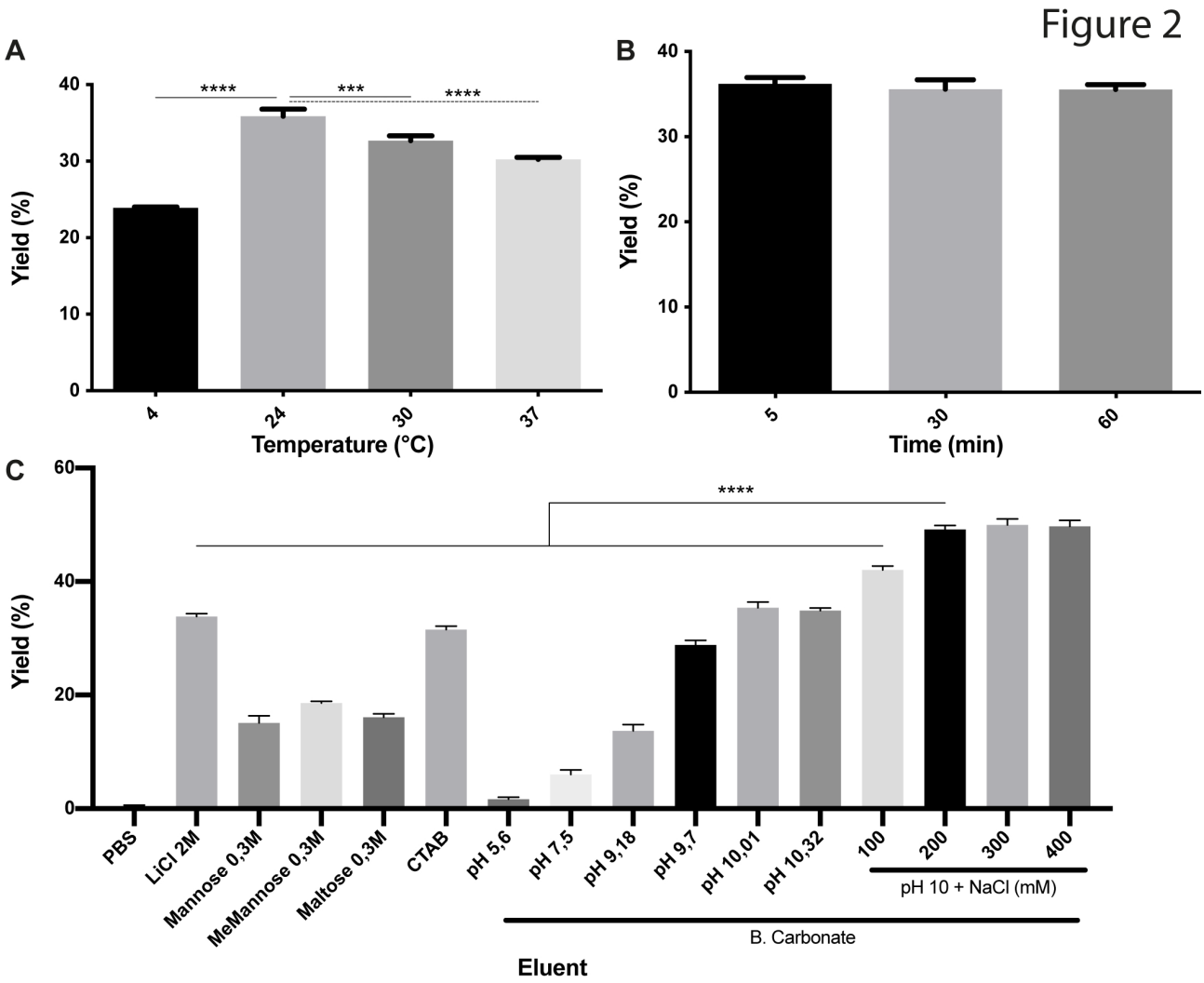

149

150 Taking into consideration the importance of this positive charge in the interaction of $SLAP_{TAG}$ with the
151 membrane-bound compound teichoic acid, a set of cationic compounds was evaluated for the elution. As
152 shown in Fig. 2C, 0.3M of CTAB was able to elute (H_6)-GFP-$SLAP_{TAG}$ with similar efficiency as the LiCl
153 solutions. Although CTAB was very efficient in this step, we found that this compound was difficult to
154 remove downstream from the elution fraction. Then, considering that $SLAP_{TAG}$ has a theoretical isoelectric
155 point (pI) value of 9.92, we explored if the modification of pH can be adapted as an elution method. As
156 shown in Fig. 2C, when the pH of the bicarbonate buffer was close to the theoretical $SLAP_{TAG}$ isoelectric
157 point (pI), (H_6)-GFP-$SLAP_{TAG}$ was efficiently eluted from BM. In addition, after establishing the bicarbonate
158 buffer at pH 10 as an elution buffer, we explore if the addition of NaCl can improve the elution process. As
159 shown in Fig. 2C, the addition of 200 mM of NaCl was able to maximize the yield of recovery of (H_6)-GFP-

160 SLAP$_{TAG}$ in the eluate. Interestingly, 200 mM of NaCl is the same concentration present in the

161 binding/washing buffer that has no effect in detaching SLAP-tagged proteins.

162 **The optimized SAC protocol allowed the efficient purification of proteins with similar efficiency to the**

163 **high-performance Ni^{2+}-charged agarose matrix (IMAC).**

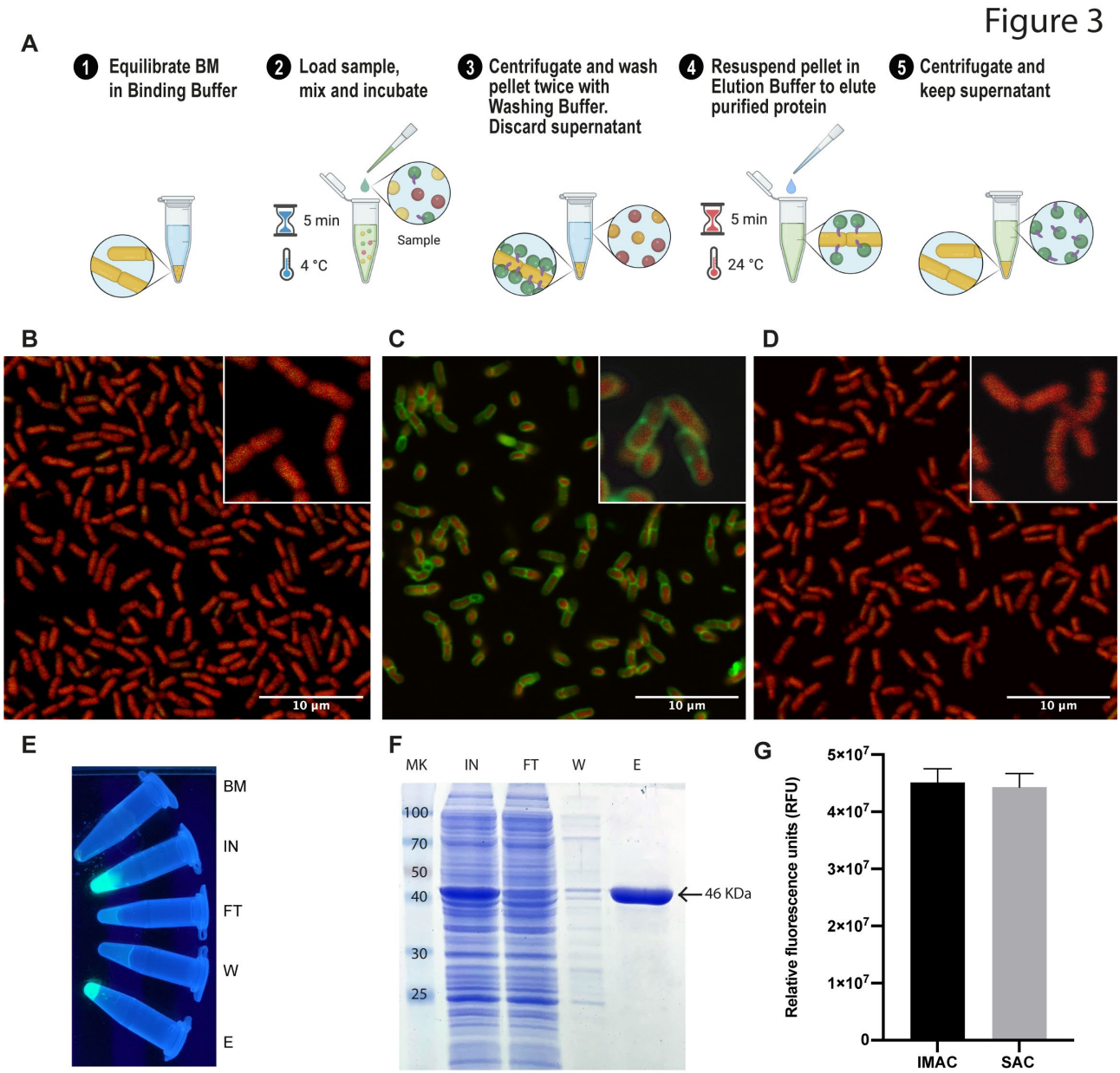

164

165 With all the experimental information obtained, an optimized SAC protocol for the purification of SLAP-

166 tagged proteins was established as shown in Fig. 3A. Remarkably, the entire process of protein purification

167 can be performed in 15 minutes. To have a direct observation of the purification process of (H_6)-GFP-

168 SLAP$_{TAG}$, the BM was fixed and immobilized on coverslips at different steps of the process of protein

169 purification to be observed by confocal microscopy. As shown in Fig. 3B, before the incubation of BM with
170 (H_6)-GFP-$SLAP_{TAG}$, only a red native autofluorescence can be observed from fixed *Bacillus subtilis* natto cells
171 present in BM. Remarkably, after the incubation of BM with (H_6)-GFP-$SLAP_{TAG,}$ it was possible to detect the
172 adhesion of the reporter protein to the BM forming a recombinant fluorescent S-layer that covers
173 completely the bacterial surface (Fig. 3C). As expected, after the addition of the elution buffer the (H_6)-GFP-
174 $SLAP_{TAG}$ was completely removed from the bacterial surface (Fig. 3D). In addition, the whole process of
175 purification can also be monitored by direct observation under UV light (Fig. 3E)

176 Since SAC was efficient in protein purification, we compared this new technique against an established
177 affinity purification protocol. For this, we took advantage of (H_6)-GFP-$SLAP_{TAG}$ also has a His-tag that can be
178 purified by a Metal-Affinity-Chromatography or IMAC. As described in Materials and Methods, a bacterial
179 lysate (H_6)-GFP-$SLAP_{TAG}$ was divided into two fractions and both protocols were performed accordingly in
180 parallel, confirming that SAC optimized protocol was able to purify (H_6)-GFP-$SLAP_{TAG}$ with high efficiency
181 (Table Supp. 1 and Fig. 3F) and with a similar yield to the one obtained with the commercial IMAC (Fig. 3G).

182 **Proteins of different biological sources, molecular weights, biochemical functions, or expressed by**
183 **procaryotic or eukaryotic expression systems can be efficiently purified by the SAC.**

184 To evaluate if $SLAP_{TAG}$ and SAC can be adapted as a universal protein purification system, a set of the
185 selected proteins were fused to the $SLAP_{TAG}$ (Fig. 4).

Figure 4

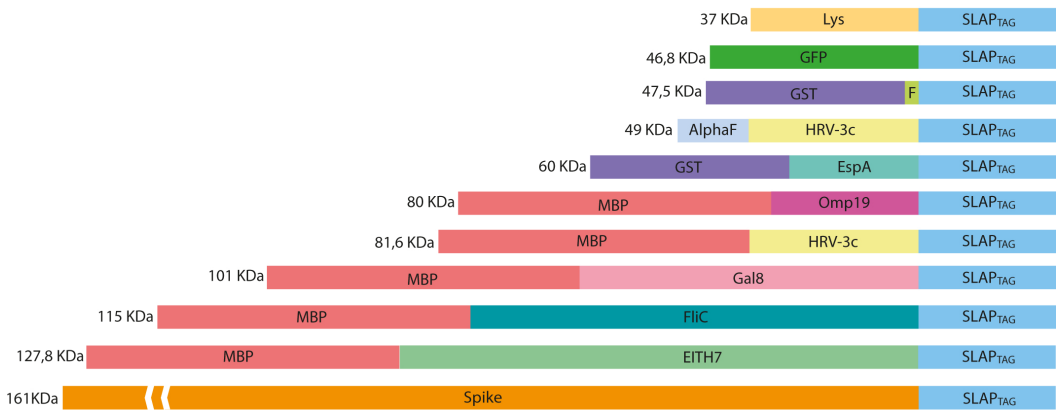

186

187 Thus, bacterial proteins like *Salmonella* flagellin (Fig.5A), the STEC proteins, EspA (Fig. 5B), the chimeric EIT

188 (Fig. 5C), the *B. abortus* Omp19 (Fig. 5D), the bacteriophage protein T7-lysozyme (Fig. 5E), the human viral

189 proteins Rhinovirus 3C Protease (Fig. 5E), the mouse Galectin-8 (Fig. 5G) and the commercial molecular tag

190 GST (Fig. 5H), were fused in frame with the $SLAP_{TAG}$.

Figure 5

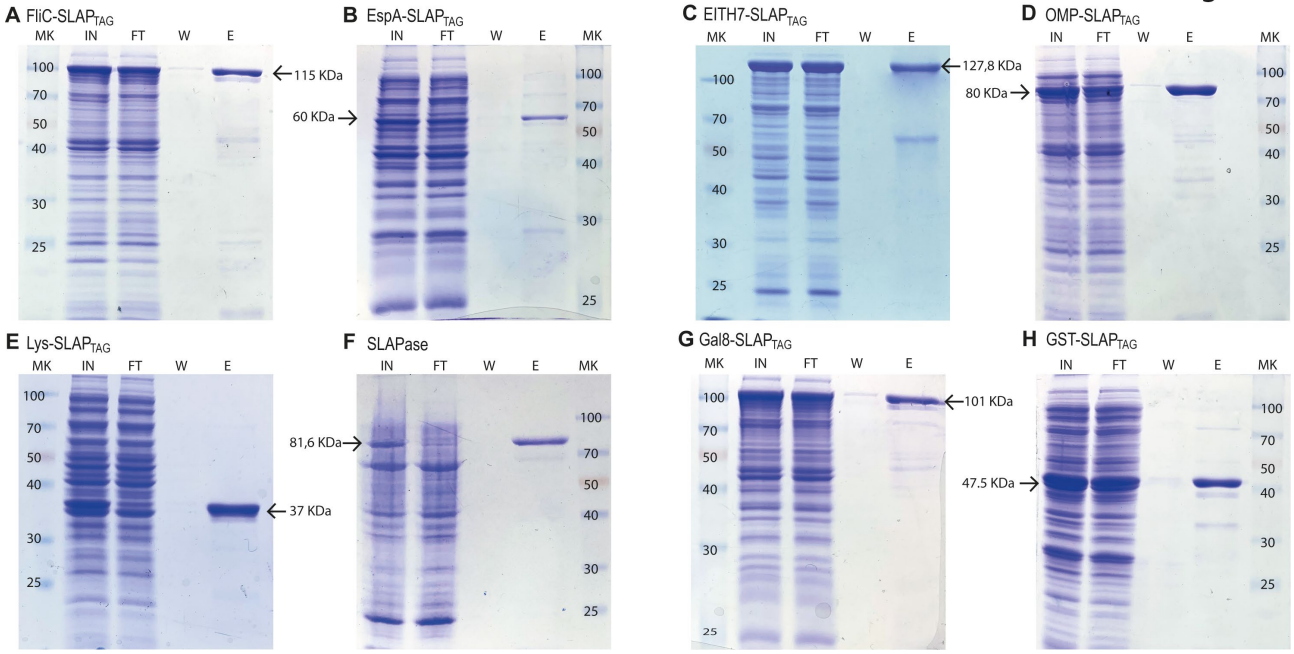

191

192 As shown in Fig. 5, all the selected proteins were purified efficiently with SAC. In addition to the bacterial

193 expression system, different protein expressions systems (yeast and mammalian cells) were also evaluated

194 (Fig. 6). As shown in Fig. 6A the viral HRV 3C protease fused to the $SLAP_{TAG}$ was expressed and purified from

195 *Pichia pastoris* supernatant. Also, the SARS-CoV2 SPIKE fused to the $SLAP_{TAG}$ was purified from the

196 supernatant of transfected HEK293 (Fig. 6B). These results confirmed that the $SLAP_{TAG}$ can be widely

197 adopted for affinity chromatography purification.

Figure 6

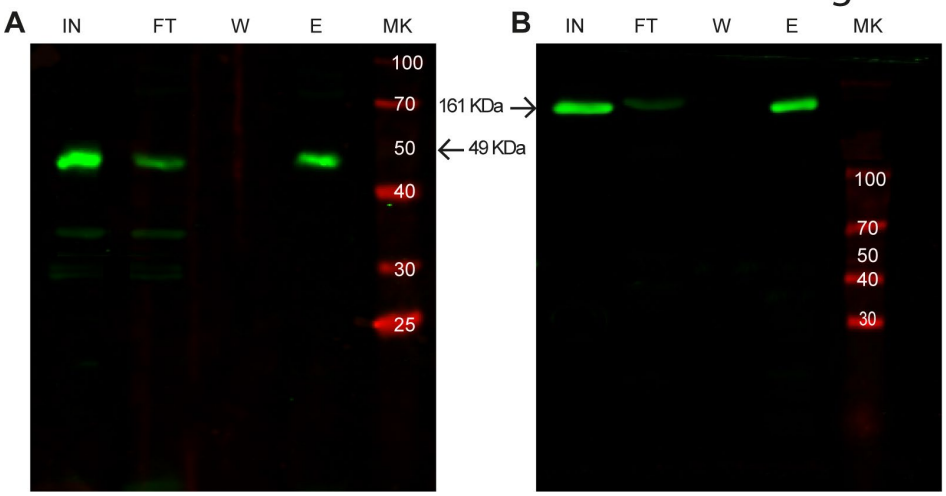

198

199 **BM is a reusable chromatography matrix with long-term stability.**

200 As described in the Methods section a batch of BM was produced, and several aliquots were frozen at -20ºC
201 to study time stability. As shown in Fig. 7A, at different times, a few aliquots were unfrozen and tested for
202 protein purification of the reporter protein (H_6)-GFP-$SLAP_{TAG}$ being the BM stable for more than a year that
203 was tested (14 months). In addition, BM reusability capacity was evaluated determining that the matrix can
204 be reused five times with no modification of the protein purification yield (Fig. 7B).

Figure 7

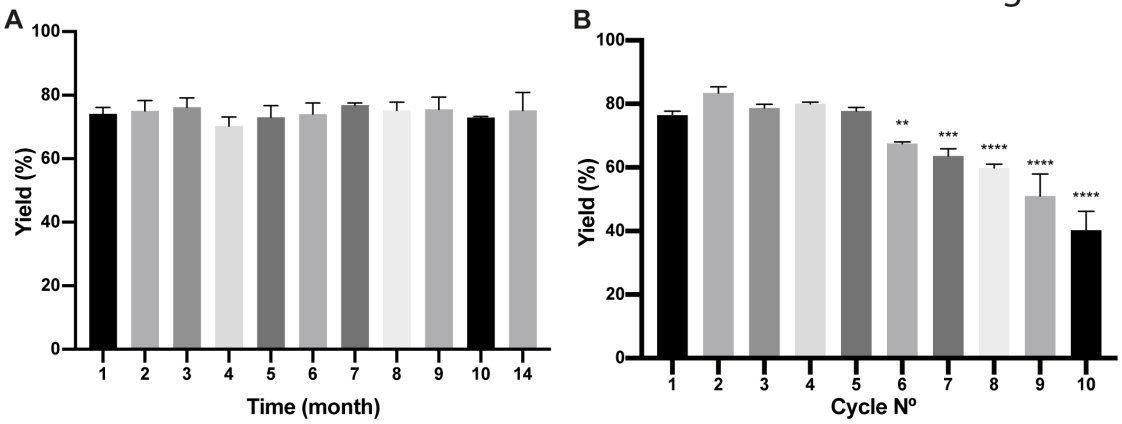

205

206 **Use of the Human Rhinovirus 3C protease fused to the $SLAP_{TAG}$ ($SLAP_{ASE}$) to release the SLAP-tagged**
207 **proteins from BM.**

208 As shown in Fig. 4 and 5 the gene sequence of the viral protease HRV-3C was fused to the $SLAP_{TAG}$ (named
209 $SLAP_{ASE}$), recombinantly expressed, and purified (Fig. 8B and 8D, lane SLAPase) to evaluate its activity. A

210 reporter protein for $SLAP_{ASE}$ activity was generated (GFP-LEVLFQGP-$SLAP_{TAG}$) (Table 1) and a protocol for tag-
211 removal by SLAPase was set as described in the Methods section. As shown in Fig. 8A the GFP-LEVLFQGP-
212 $SLAP_{TAG}$ was expressed (Fig 8B and Fig. 8C, lane Input or IN) and mixed with the BM for 5 minutes allowing
213 the binding process. After binding, a purified $SLAP_{ASE}$ was added to the mix and incubated for 60 minutes
214 releasing a tag-less GFP (Fig. 8B and Fig 8C, Fig 8E, lanes flow-through or FT) by proteolysis. Cut $SLAP_{TAG}$ is
215 not observed in the flow-through indicating that was retained by the BM along with the SLAPase. To confirm
216 these steps, post-proteolysis BM was incubated with LiCl solution to recover any residual bound SLAP-
217 tagged protein. As shown in Fig. 8B and 8D (lane Elution or E), the LiCl solution released the SLAPase and
218 the cut $SLAP_{TAG}$.

Figure 8

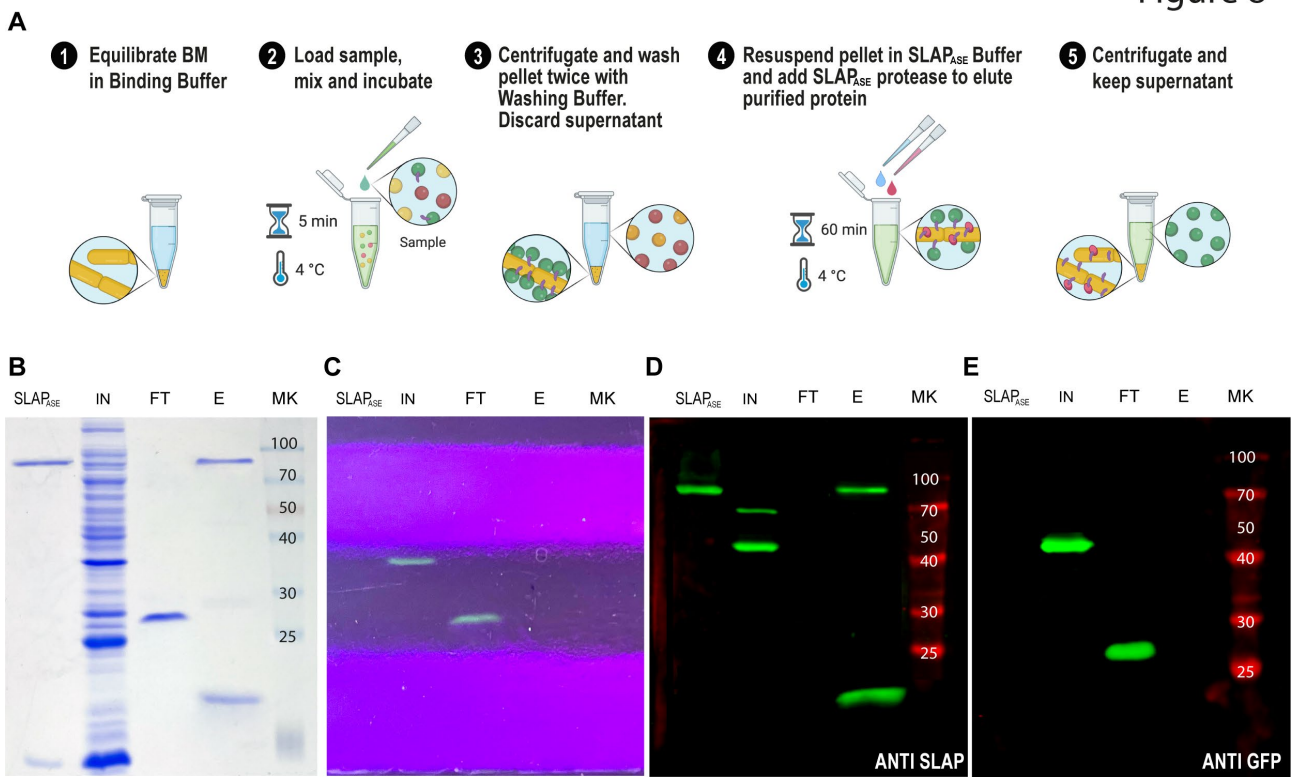

219

220 **Adaptation of SAC to magnetic affinity chromatography.**

221 Since we confirmed the efficiency and universality of SAC for the purification of recombinant proteins, we
222 explored a magnetic affinity chromatography alternative for SAC (Fig. 9A). As shown in Fig. 9B, 9C, and
223 Supplementary Video-1 the (H_6)-GFP-$SLAP_{TAG}$ was purified in a few and easy steps. As shown in the SDS-

224 PAGE (Fig. 9B) the adapted SAC protocol for magnetic chromatography (BM_{mag}) was able to purify the
225 reporter protein (H_6)-GFP-$SLAP_{TAG}$ very efficiently (Fig. 9B, lane Elution or E). Interestingly, this protocol can
226 be adapted to commercial devices that use magnetic force for protein or DNA purification (like King Fisher
227 Flex from ThermoFisher). In Fig. 9C the entire process of purification was monitored by direct observation
228 under UV light (Supp. video 1). Noteworthy, the binding of the BM_{mag} to GFP quenched the fluorescence of
229 this protein, an effect that was described for transition metal binding to GFP or binding of iron cations to
230 fluorescent proteins (Fig. 9C, tube IN+BM_{mag}) [19,20].

231

Figure 9

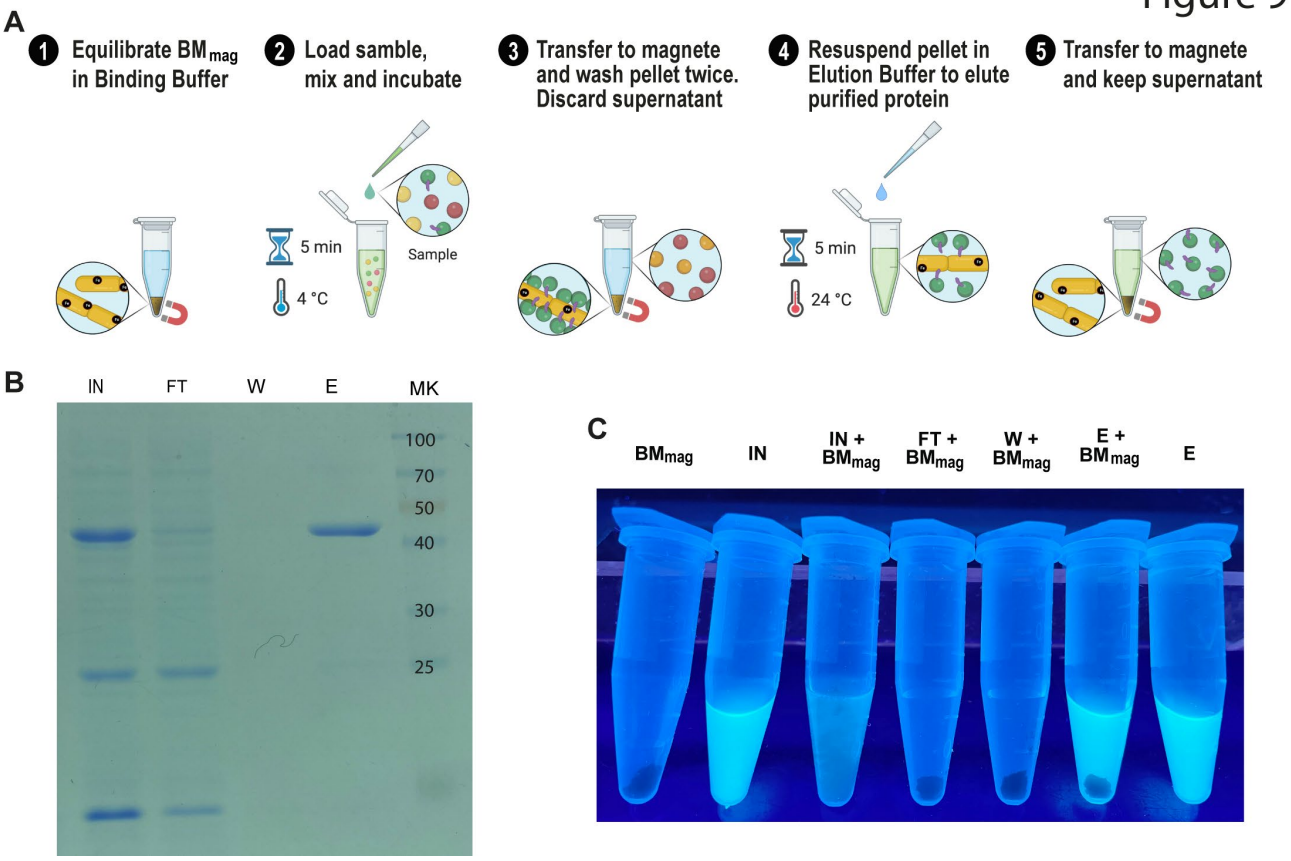

232
233
234

235 **Discussion**

236 The *B. subtilis-derived* matrix, named here as Bio-Matrix (BM), showed a high performance in its binding
237 and elution capacities, combined with good purification parameters for our reporter protein (H_6)-GFP-
238 $SLAP_{TAG}$. Results presented here show that the SAC protocol can be potentially adapted as a universal tool
239 for recombinant protein purification. Thus, proteins from different origins, with different molecular
240 weights, or produced by different recombinant expression systems (bacteria, yeast, or cells) can be
241 efficiently purified by SAC. In addition to its universal application, we demonstrate here that SAC was able
242 to achieve a protein yield similar to those obtained by commercial affinity chromatography systems such
243 as the Immobilized Metal Affinity Chromatography or IMAC. As reported, in protein production bioprocess,
244 chromatography is the most expensive step[21]. Of interest, the SAC protocol only uses simple and low-cost
245 reagents, consequently presenting an economic advantage in protein purification over current commercial
246 systems. In addition, since the Biomatrix is "grown" instead of being chemically synthesized, the production
247 of larger quantities of chromatography matrix can be achieved easily by simply scaling up the volume of the
248 bioreactor. In addition, small research labs can easily produce their version of the in-house of BM by the
249 protocol provided here.

250 One critical step in the generation of the affinity matrix is the immobilization of the affinity ligand to the
251 chromatography matrix. Initially, at the beginning of the affinity chromatography development, the
252 immobilization of affinity ligands was performed by covalent modification using diazo coupling [11]. This
253 procedure allows to immobilize different haptens or certain proteins to isolate antibodies. A second
254 breakthrough in affinity chromatography was the development of the cyanogen bromide (CNBr)
255 immobilization method which allows the easy cross-link of proteins or peptides to the activated agarose
256 matrix[11]. These two major advances were combined in 1969 by Cuatreacasas et al where the term affinity
257 chromatography was used for the first time [22].

258 In contrast, in Bio-Matrix affinity ligands (LTA and teichoic acid) are naturally integrated into the surface of
259 the BM [17] and consequently, no chemical reactions to cross-link the affinity ligands to BM are required.
260 Remarkably, no toxic chemicals or solvents are required in BM production.

261 From all the supports used as a matrix in affinity chromatography [11], the polysaccharide agarose is the most
262 frequently used due to its low cost, large pores size, very low non-specific binding, and great stability over
263 a broad pH range. However, agarose has limited mechanical stability at high operating pressures that limit
264 the use of this matrix as support in high-performance liquid chromatography (HPLC) [11]. Initially, other
265 polysaccharides have also been adapted as supports in affinity chromatography like cellulose. Although
266 cellulose displays a lower surface area and mechanical stability than agarose because of its low back
267 pressure is a very useful tool used in preparative chromatography at high flow rates when used in
268 membrane-based affinity separations[11]. In addition, carbohydrate-based supports combined with high-
269 dense core material such as quartz, have been adapted in expanded-bed adsorption (EBA) chromatography
270 [11]. Expanded-bed adsorption (EBA) chromatography is an excellent option for the capture of proteins
271 directly from unclarified crude samples (such as a CHO cell supernatant)[23]. In EBA, the chromatography
272 matrix (chromatographic bed) is initially expanded by an upward flow of the equilibration buffer[24]. A crude
273 sample, that might have a mixture of soluble proteins, contaminants, entire cells, and cell debris along with
274 the protein of interest (POI) is then passed upward through the expanded bed. In this process, POIs are
275 captured on the adsorbent, while undesired particulates, aggregates, and contaminants pass through [24].
276 Then, the replacement of binding buffer/washing buffer by an upward flow of elution buffer will result in
277 POI desorption. Finally, when the flow is reversed, the adsorbent particle can be separated by
278 sedimentation and desorbed POI can be recovered for further purification steps[24].

279 EBA has been demonstrated to be a useful method, particularly for protein capture in a continuous protein
280 purification process from unclarified feedstocks[25] in the recovery of enzymes and therapeutic proteins from
281 a variety of expression hosts[25]. Interestingly, the use of liquid magnetically stabilized fluidized beds (MSFBs)
282 has been explored for EBA [26]. Magnetically susceptible chromatography supports are forced to low back-

283 mixing by applying a weak, external magnetic field that oriented the magnetic particles axially or
284 transversely relative to the flow [25]. This technique also gives great opportunities for process integration by
285 achieving particulate removal and the capture of the product desired in a single operation[25] [26].

286 As shown here, SAC is an adsorption affinity chromatography, that was able to efficiently capture SLAP-
287 tagged proteins directly from different feeds like bacterial lysates, *Pichia pastoris* supernatant, or HEK293
288 cells supernatant in a single step. In addition, a magnetically susceptible biomatrix was generated that still
289 was able to capture SLAP-tagged proteins. Both results made SAC an interesting technique for EBA or
290 EBA/MSFBs adaptation.

291 In the last decade, the introduction of single-use technologies has enlightened the potential for reduced
292 regulatory and operational costs associated with chromatography. The researchers point to its potential for
293 simpler operation, shorter processing times, and decreased buffer consumption, leading to better
294 economics. [27]. Also, the lack of need for cleaning over repeat-use cycles significantly reduces costs. SAC
295 could be a single-use alternative chromatography for some industries, with the benefit of being more eco-
296 friendly than those available on the market, as it is a biologically based and biodegradable matrix.

297 SAC proved to successfully adapt to protease tag removal. Although new technologies are being developed
298 for tag removal (e.g., inteins), the enzymatic cleavage of the tag is still preferred as it is the most controlled
299 process, with no premature cleaving and the best yields are obtained[28]. Moreover, new technologies might
300 be compatible with SAC.

301 Therefore, we propose that $SLAP_{TAG}$ affinity chromatography for protein purification in industries with
302 permissive regulations. SAC can be adapted as an in-house protein purification system, available for any
303 laboratory around the globe, to produce pure recombinant proteins for research, diagnosis, and the food
304 industry. Although so far regulatory issues might preclude the use of the SAC for proteins used as
305 biotherapeutics, new efforts have been performed to develop a new version of matrix chromatography
306 suitable for more stringent industrial or clinical purposes.

307

308 **Methods**

309 ***Strains and plasmids.*** All the bacterial strains and plasmids used here were summarized in Table 1. Bacteria
310 *Escherichia coli* and *Bacillus subtilis* strains were grown in Luria Bertani (LB) medium (Sigma, St. Louis, MO,
311 United States) at 37ºC and 180 rpm. Bacterial plasmid vectors were transformed into *E. coli* DH5α or *E. coli*
312 BL21 (DE3) for protein expression. *Pichia pastoris* was grown in Yeast Extract–Peptone–Dextrose
313 (YPD) medium at 28ºC 180 rpm. HEK293F cells were maintained at 37ºC in a 5% CO2 atmosphere in Dulbecco
314 modified Eagle medium (DMEM) supplemented with 5% fetal bovine serum and streptomycin (50 µg/ml)-
315 penicillin (50 U/ml). The SARS-CoV-2 Spike ectodomain Hexa-pro construction (Table 1) was a gift from Jason
316 McLellan (Addgene # 154754; http://n2t.net/addgene:154754;RRID: addgene_154754)[29].

317 ***Cloning***

318 Lysozyme gene was amplified from the pLysS plasmid (Millipore Sigma-Novagen) with the oligonucleotide
319 primers Fw-lys-*Nde*I (CCCATATGGCTCGTGTACAGTTTAAACAACGTG) and Rv-lys-SalI
320 (CGGTCGACTCCACGGTCAGAAGTGACCAGTTCG). The PCR product was digested with the restriction enzymes
321 *Nde*I and *Sal*I and then cloned into the pLC3-EITH7-SlpA vector in the same restriction sites and the
322 recombinant plasmid was transformed into *E. coli* DH5α. In addition, the lysozyme gene was subcloned into
323 pET28-e GFP-SlpA at the *Nde*I and *Not*I restriction sites and transformed into *E. coli* BL21 by electroporation.

324 *EspA* gene was amplified with the following primers: *pRvEspAXbaI* (GCTCTAGATTTACCAAGGGATATTGCTG)
325 *and pFwEITSalI* (ACGCGTCGACGATATGAATGAGGCATCTAAA). After digestion with *Xba*I and *Sal*I, the gene was
326 cloned into *pGEX-SlpA* (Table 1), which was previously digested with the same enzymes. The plasmid was
327 introduced by electroporation into *E. coli* BL21.

328 The *have-3c-slap tag* gene was synthesized and cloned in pMAL-c5X and pPICZalfa-B for protein expression
329 in *E. coli* and *P. pastoris* respectively (Gene Universal, Delaware-USA).

330 For *P. pastoris* GS115 transformation, 5µg of pPICZalfa B – *hrv-3c* plasmid was linearized with *Sac*I restriction
331 enzyme and transformed into cells through electroporation using 2 mm gap cuvettes (1500 V, 125 X, 50 lF).
332 Transformed cells were selected by plating on a YPD medium containing Zeocin 100ug/ml for resistance
333 selection. Isolated colonies were further grown in test tubes containing YPD broth and after 24 h, protein
334 expression was induced by adding 1% (v/v) pure methanol every 24 h. Supernatants were sampled after 72
335 h of induction and the best producer clones were chosen for further experiments.

336 The pET28-eGFP-SLAP was digested with *BamH*I and *Xho*I restriction enzymes and the $SLAP_{TAG}$-containing
337 band was subcloned into SARS-CoV-2 S HexaPro plasmid (Addgene#154754) with the same restriction sites.

338 ***Protein expression***

339 *E. coli* BL21 were grown at 37ºC 180 rpm in liquid LB supplemented with antibiotics until they reached OD_{600}
340 = 0.6. Then, 0.1 mM IPTG was added, and bacteria were grown for another 20 hours at 18ºC 180 rpm. Finally,
341 bacteria were harvested and lyzed by sonication. The bacterial lysates were clarified by centrifugation.

342 *For Pichia, pastoris* protein expression cells were induced with methanol. Briefly, *P. pastoris* cultures were
343 grown in 50 ml of YPD for 48 h. until the dextrose was consumed. Then, methanol pulses (200ul) were
344 supplied every 24 h for 5 days. Finally, *P. pastoris* were harvested, and supernatants were collected.

345 HEK293 cells were transfected using polyethyleneimine (PEI) for protein expression. Briefly, thirty thousand
346 cells per well were seeded in 24 well plates and incubated at 37 ℃, 5% CO_2 for 24 h. For transfection, 4µl of
347 PEI was diluted in 40µl of DMEM. 500 ng of DNA was added, and the transfection mix was incubated for 20
348 min at room temperature. Then, the transfection mix was transferred to the cells and incubated for 48 h.
349 Finally, the supernatant was collected to check protein expression.

350 ***6xHis-Tag purification method***

351 Purification of 6xHis-tagged proteins was carried out according to the manufacturer's protocol. Briefly,
352 benchtop columns were equilibrated with the binding buffer (200 mM NaCl, 50 mM Tris-HCl pH 7.5). Columns
353 were loaded with the bacterial lysate. After being washed, columns were eluted in steps with 10, 50-, 100-,
354 300-, and 500-mM imidazole in the equilibration buffer. When compared with the SAC, the IMAC batch
355 format was adopted. Thus, Ni-NTA superflow resin (Qiagen) was equilibrated with buffer (200 mM NaCl, 50
356 mM Tris-HCl pH 7.5) in 1,5 ml tubes. Cleared bacterial lysates were loaded and mixed in an orbital shaker for
357 1 hour at 4ºC. Samples were centrifugated and, after being washed, the resin was eluted with 500 mM
358 imidazole in an equilibration buffer.

359 ***Bio-Matrix preparation***

360 *B. subtilis* natto was grown in 200 mL of Luria-Bertani broth at 37ºC 180 rpm for 48 hrs. Then, the culture was
361 centrifugated and the bacteria were washed twice with PBS. The culture was resuspended in PBS with 2%
362 glutaraldehyde and incubated overnight with soft agitation. Next, fixed bacteria were washed twice with PBS
363 and stored in 20 % ethanol. 1mL of BM correspond to DO600=30 of B. subtilis.

364 BM was weighted in a drying scale (KERN MLS-D) and a calibration curve for dry weight vs optical density was
365 performed.

366 ***SLAP$_{TAG}$ purification method***

367 To purify the SLAP-tagged proteins, BM was equilibrated in binding buffer (200 mM NaCl, 50 mM Tris-HCl pH
368 7.5). Then, samples were incubated with the BM at different times and temperatures. Samples were
369 centrifuged (8000 rpm) and the BM was washed 3 times with binding buffer. Finally, samples were incubated
370 at different times and temperatures with the corresponding solution for elution. Proteins expressed in
371 HEK293 and *P. pastoris* were purified from the supernatant with the final protocol described in this paper.

372 ***Biomatrix time stability and reusability*.**

373 To analyze stability in time, aliquots of BM were frozen at -20ºC. At different times, samples were unfrozen
374 and used for purifying GFP-SLAP following the protocol developed in this paper. To analyze reusage, an
375 aliquot of BM was used for purifying GFP-SLAP following the protocol developed in this paper. After elution,
376 the BM was washed with two volumes of elution Buffer (Bicarbonate Buffer pH 10, 200 mM NaCl) and then
377 two volumes of binding buffer (200 mM NaCl, 50 mM Tris-HCl pH 7.5). The cleaning process was repeated
378 each time after elution.

379 ***Protein analysis***

380 Protein samples were dissolved in a cracking buffer and incubated for 5 min at 100ºC. Protein electrophoresis
381 was performed at 120V on 12% SDS-PAGE gel. Gels were stained in a Coomassie-Blue solution (20%
382 methanol, 10% acetic acid).

383 For Western Blot analysis, proteins were transferred to a nitrocellulose membrane for 55 min at 15V using a
384 semi-dry electroblotting transfer unit (Bio-Rad, Hercules, CA, United States). Membranes were incubated for
385 1 hour with blocking buffer (1% dry skim milk, 0,1% Tween in PBS). Then, membranes were incubated for 1
386 hour with primary antibody diluted in blocking buffer (1/500). After washing with PBS-0,1% Tween,
387 membranes were incubated for 1 hour with IRDye fluorophore-labeled secondary antibodies (LI-COR, Lincoln,
388 NE, United States) diluted in a blocking buffer (1/20000). Finally, membranes were scanned using the Odyssey
389 Imaging System (LI-COR).

390 ***Fluorescence measurements***

391 GFP fluorescence measurements were performed at 485/535nm excitation-emission wavelength
392 respectively using FilterMax F5 Microplate Reader in Black 96 Well Plates (Thermo).

393 ***Protein modeling***

394 (H_6)-GFP-SLAP$_{TAG}$ structure was predicted by AlphaFold[13]. ColabFold web interface was employed using
395 standard settings (five models and no templates).

396 ***Adsorption isotherm***

397 Adsorption isotherms for (H_6)-GFP-SLAP$_{TAG}$ on BM were performed using batch experiments. BM was
398 equilibrated with binding buffer (50 mM Tris-HCl, 200 mM NaCl, and pH 7.6). Purified (H_6)-GFP-SLAP$_{TAG}$
399 protein at 3 mg/ml in binding buffer was used as a stock solution. Different concentrations of protein were
400 incubated with 10 µl of BM. After reaching equilibrium, samples were centrifugated and GFP fluorescence
401 from the supernatant was measured. Unbound protein in equilibrium with the BM was calculated using GFP
402 fluorescence. Bound protein was estimated by the difference between input and unbound protein. The
403 adsorption isotherm data were then fitted to the Langmuir isotherm equation to calculate the parameters
404 Qmax and K_D.

405 ***Confocal Fluorescence Microscopy***

406 Samples were incubated for 30 min in plates treated with poly-L-Lysine (Sigma, St. Louis, MO, United State).
407 After treatment with PFA (4% in PBS), samples were washed twice with PBS. Finally, samples were observed
408 with a confocal laser-scanning microscope Olympus FV1000 using a PlanApo N (60 × 1.42 NA) oil objective.

409 ***Cleavage of SLAP$_{TAG}$ with SLAP$_{ASE}$ protease***

410 Cleavage buffer recommended for commercial HRV3c protease was prepared: 50 mM Tris-HCl, pH 7.0, 150
411 mM NaCl, 1 mM EDTA, and 1 mM dithiothreitol. GFP-LEVLFQGP-SLAP$_{TAG}$ protein was bound to the BM. After
412 binding BM was washed with the same buffer thrice at 4ºC. SLAP$_{ASE}$ was added and incubated at 4ºC.
413 Percolate containing GFP protein without SLAP$_{TAG}$ was recovered. As a control, the protease and SLAP$_{TAG}$ were
414 eluted with Bio-Matrix elution buffer after cleavage.

415 ***Synthesis of iron nanoparticles***

416 Iron nanoparticles were synthesized by reverse co-precipitation as described by Nadi et al [30]. In summary,
417 the precursor was prepared by dissolving 0.89 g of FeCl2.4H2O in 90 mL of water. The sample was incubated
418 in stirring for 15 min and sonicated for 10 min to ensure complete dissolution of the salt. The solution was
419 then poured over a solution of ammonium hydroxide diluted 1:2 with water and stirred for an hour. Finally,
420 the sample was washed repeatedly with deionized water.

421 ***Magnetic Bio-Matrix generation***

422 Briefly, 5 ml of Bio-Matrix were resuspended in PBS and iron nanoparticles were added at a final
423 concentration of 40 g/L. The sample was mixed with gentle stirring for 30 minutes. Then, it was washed
424 repeatedly with PBS 1X and preserved in 20% ethanol.

425 ***Antibody generation***

426 Mice were intraperitoneally injected with 10µg of purified GST-SLAP$_{TAG}$ or GFP in aluminum hydroxide (Imject
427 Alum ThermoFisher). Two and four weeks later, booster doses of 5µg of protein were administrated.

428 ***Statistical analysis***

429 Statistical analyses were performed using GraphPad Prism 9 software. Statistical significance was analyzed
430 by one-way ANOVA with Bonferroni.

431 **Acknowledgments**

432 We would like to thank Dr. Juan E. Ugalde for his careful and critical reading of this manuscript.

433 This work was supported by grants from the Agencia Nacional de Promoción Científica y Técnológica,
434 Buenos Aires, Argentina, PICT-2018-0778, PICT-2021-CAT-I-00049 and CONICET (PUE-0086). E.J.M., P.J.U.,
435 and C. M. D. are doctoral fellows from CONICET. MVP is a postdoctoral fellow from the Agencia Nacional de
436 Promoción Científica y Tecnológica. M.S.R. and G.B. are members of the Research Career of CONICET.

437 **Availability of materials and data**

All data generated or analyzed during this study are included in this published article and its supplementary information files.

441 **References**

442 1. Wood, E. J. Nature's robots: A history of proteins. *Biochem. Mol. Biol. Educ.* **32**, 282–282 (2004).

443 2. Buxbaum, E. *Enzymes Are Biocatalysts*. *Fundamentals of Protein Structure and Function* (2015).
444 doi:10.1007/978-3-319-19920-7_4.

445 3. Baldo, B. A. Chimeric Fusion Proteins Used for Therapy: Indications, Mechanisms, and Safety. *Drug*
446 *Saf.* **38**, 455–479 (2015).

447 4. Fei Wen, Sheryl B. Rubin-Pitel, and H. Z. Engineering of Therapeutic Proteins.Chp7. 153–177 (2009).

448 5. Schales, O. Preparation and Properties of Renin. *J. Am. Chem. Soc.* **64**, 561–564 (1942).

449 6. Wood, D. W. New trends and affinity tag designs for recombinant protein purification. *Curr. Opin.*
450 *Struct. Biol.* **26**, 54–61 (2014).

451 7. Freitag, R. & Horváth, C. Chromatography in the downstream processing of biotechnological
452 products. *Adv. Biochem. Eng. Biotechnol.* **53**, 17–59 (1996).

453 8. Kuntz, I. D., Chen, K., Sharp, K. A. & Kollman, P. A. The maximal affinity of ligands. *Proc. Natl. Acad.*
454 *Sci. U. S. A.* **96**, 9997–10002 (1999).

455 9. Mouratou, B., Béhar, G. & Pecorari, F. Artificial affinity proteins as ligands of immunoglobulins.
456 *Biomolecules* **5**, 60–75 (2015).

457 10. Hais, I. M. Biospecific sorption, Prague, 1910: Emil Starkenstein (1884-1942). *J. Chromatogr. B*
458 *Biomed. Sci. Appl.* **376**, 5–9 (1986).

459 11. Rodriguez, E. L. *et al.* Affinity chromatography: A review of trends and developments over the past
460 50 years. *Journal of Chromatography B: Analytical Technologies in the Biomedical and Life Sciences*
461 vol. 1157 at https://doi.org/10.1016/j.jchromb.2020.122332 (2020).

462 12. Uriza, P. J. *et al.* Development of an Antigen Delivery Platform Using Lactobacillus acidophilus

463 Decorated With Heterologous Proteins: A Sheep in Wolf's Clothing Story. *Front. Microbiol.* **11**,
464 (2020).

465 13. Jumper, J. *et al.* Highly accurate protein structure prediction with AlphaFold. *Nature* **596**, 583 (2021).

466 14. Garduno, R. A., Phipps, B. M. & Kay, W. W. Physical and functional S-layer reconstitution in
467 Aeromonas salmonicida. *J. Bacteriol.* **177**, 2684–2694 (1995).

468 15. Mader, C., Huber, C., Moll, D., Sleytr, U. B. & Sára, M. Interaction of the Crystalline Bacterial Cell
469 Surface Layer Protein SbsB and the Secondary Cell Wall Polymer of Geobacillus stearothermophilus
470 PV72 Assessed by Real-Time Surface Plasmon Resonance Biosensor Technology. *J. Bacteriol.* **186**,
471 1758–1768 (2004).

472 16. Li, J., Hu, X., Yan, J. & Yuan, Z. Species-specific cell wall binding affinity of the S-layer proteins of
473 mosquitocidal bacterium Bacillus sphaericus C3-41. *Appl. Environ. Microbiol.* **75**, 3891–3895 (2009).

474 17. Lortal, S. *et al. S-layer of Lactobacillus helveticus atcc 12046: isolation, chemical characterization and*
475 *re-formation after extraction with lithium chloride Slayer of Lactobacillus helveticus ATCC 12046:*
476 *isolation, chemical characterization and re-formation after extraction with lithium chloride*. *Society*
477 *for General Microbiology* vol. 138 https://hal.inrae.fr/hal-02713428 (1992).

478 18. Fina Martin, J. *et al.* Exploring lectin-like activity of the S-layer protein of Lactobacillus acidophilus
479 ATCC 4356. *Appl. Microbiol. Biotechnol.* **103**, 4839–4857 (2019).

480 19. Kim, I. J., Xu, Y. & Nam, K. H. Spectroscopic Analysis of Fe Ion-Induced Fluorescence Quenching of
481 the Green Fluorescent Protein ZsGreen. *J. Fluoresc.* **31**, 307–314 (2021).

482 20. Richmond, T. A., Takahashi, T. T., Shimkhada, R. & Bernsdorf, J. Engineered metal binding sites on
483 green fluorescence protein. *Biochem. Biophys. Res. Commun.* **268**, 462–465 (2000).

484 21. Wong, F. W. F., Ariff, A. B. & Stuckey, D. C. Downstream protein separation by surfactant
485 precipitation: a review. *Crit. Rev. Biotechnol.* **38**, 31–46 (2018).

486 22. Cuatrecasas, P., Wilchek, M. & Anfinsen, C. B. Selective enzyme purification by affinity
487 chromatography. *Proc. Natl. Acad. Sci. U. S. A.* **61**, (1968).

488 23. Chase, H. A. Purification of proteins by adsorption chromatography in expanded beds. *Trends*
489 *Biotechnol.* **12**, 296–303 (1994).

490 24. Hjorth, R., Leijon, P., Frej, A. K. B. & Jägersten, C. Expanded Bed Adsorption Chromatography. *Biosep.*
491 *Bioprocess.* 199–226 (2008) doi:10.1002/9783527619641.ch9.

492 25. Schneider, A., Herlevi, L. M., Guo, Y. & Fernandez Lahore, H. M. Perspectives on adsorption
493 technology as an effective strategy for continuous downstream bioprocessing. *J. Chem. Technol.*
494 *Biotechnol.* **97**, 2305–2316 (2022).

495 26. Tong, X. D. & Sun, Y. Application of Magnetic Agarose Support in Liquid Magnetically Stabilized
496 Fluidized Bed for Protein Adsorption. *Biotechnol. Prog.* **19**, 1721–1727 (2003).

497 27. Hester, J. F., Lu, X., Calhoun, J. D., Hochstein, R. A. & Olson, E. J. Orthogonal pre-use and post-use
498 efficiency testing for single-use anion exchange chromatography. *J. Chromatogr. A* **1654**, 462445
499 (2021).

500 28. Pina, A. S., Batalha, Í. L. & Roque, A. C. A. Affinity tags in protein purification and peptide
501 enrichment: An overview. *Methods Mol. Biol.* **1129**, 147–168 (2014).

502 29. Hsieh, C.-L. *et al.* Structure-based design of prefusion-stabilized SARS-CoV-2 spikes. *Science (80-.).*
503 **369**, 1501–1505 (2020).

504 30. Nadi, A. *et al.* Immobilisation of bacteria onto magnetic nanoparticles for the decolorisation and
505 degradation of azo dyes. *IET Nanobiotechnology* **13**, 144–149 (2019).

506

507 **Figures legends**

508 **Figure 1: Characterization of (H_6)-GFP-SLAP$_{TAG}$ binding to Bio-matrix.** (A) The AlphaFold2 model of (H_6)-GFP-
509 SLAP$_{TAG}$ fusion protein. AlphaFold2 predicted structure was automatically colored by the pLDDT confidence
510 measure. High accuracy is colored in blue while low accuracy is in red. Although SLAP$_{TAG}$ has not been
511 crystallized, structure prediction showed a good performance. (B) Figure compares (H_6)-GFP-SLAP$_{TAG}$
512 purification yield of SLAP$_{TAG}$-based affinity chromatography for different temperatures of the binding process.
513 (C) Figure compares (H_6)-GFP-SLAP$_{TAG}$ purification yield of SLAP$_{TAG}$-based affinity chromatography for
514 different times of binding incubation. (D) Adsorption isotherm of (H_6)-GFP-SLAP$_{TAG}$ onto Bio-Matrix. Asterisk
515 (****) denotes significant differences using the ANOVA method, Bonferroni test ($p < 0.0001$).

516 **Figure 2: Characterization of (H_6)-GFP-SLAP$_{TAG}$ elution.** (A) Figure compares (H_6)-GFP-SLAP$_{TAG}$ purification
517 yield of SLAP$_{TAG}$-based affinity chromatography for different temperatures of elution. (B) Figure compares
518 (H_6)-GFP-SLAP$_{TAG}$ purification yield of SLAP$_{TAG}$-based affinity chromatography for different times of elution
519 incubation. (C) Figure compares (H_6)-GFP-SLAP$_{TAG}$ purification yield of SLAP$_{TAG}$-based affinity chromatography
520 system for different eluents. The asterisk denotes significant differences using the ANOVA method, the
521 Bonferroni test (*** $p = 0{,}0003$; **** $p < 0.0001$).

522 **Figure 3: Optimized protocol for (H_6)-GFP-SLAP$_{TAG}$ purification using the Bio-matrix and comparison with**
523 **the high-performance Ni^{2+}-charged agarose matrix**. (A) Graphical description of the SLAP$_{TAG}$-based affinity
524 chromatography protocol. (B) Confocal microscopy of the Bio-Matrix. *Bacillus subtilis* red native
525 autofluorescence is observed. (C) Confocal microscopy of (H_6)-GFP-SLAP$_{TAG}$ bound to the Bio-Matrix. GFP is
526 visualized on the *Bacillus* surface. (D) Confocal microscopy of the Bio-Matrix after elution of (H_6)-GFP-SLAP$_{TAG}$.
527 (E) Tubes containing purification fractions seen under UV light. GFP input fluorescence is recovered in the
528 eluate. (F) Coomassie blue staining analysis of (H_6)-GFP-SLAP$_{TAG}$ scaled purification. BM = Bio-Matrix; MK =
529 protein marker (kDa); IN = input; FT = flowthrough; W = wash; E = elution. (G) Immobilized metal affinity
530 chromatography (IMAC) and SLAP$_{TAG}$-based affinity chromatography systems are compared in their capacity

531 to purify (H_6)-GFP-SLAP$_{TAG}$. Relative fluorescence of total (H_6)-GFP-SLAP$_{TAG}$ recovered in elution fraction is
532 shown.

533 **Figure 4: Representation of SLAP-tagged recombinant protein structure.** Lys = bacteriophage T4 lysozyme;
534 GFP = *Aequorea victoria* green fluorescent protein; GST = glutathione-s-transferase; HRV-3c = human
535 Rhinovirus 3C Protease; EspA = *E. coli* EspA protein; Omp19 = *B. abortus* Omp19 protein; MBP = maltose-
536 binding protein; Gal8 = mouse Galectin-8; EITH7 = EspA, Intimin and Tir fusion protein from the Shiga-toxin
537 producing *E. coli*; Spike = SARS-CoV2 Spike protein.

538 **Figure 5: Analysis of different SLAP-tagged protein purifications expressed in *E. coli*.** Coomassie Blue stained
539 SDS-PAGE of purification fractions of SLAP$_{TAG}$-based affinity chromatography for (A) FliC-SLAP$_{TAG}$ (B) EspA-
540 SLAP$_{TAG}$ (C) EITH7-SLAP$_{TAG}$ (D) Omp19-SLAP$_{TAG}$ (E) Lys -SLAP$_{TAG}$ (F) SLAP$_{ASE}$ (human rhinovirus 3c fused to
541 SLAP$_{TAG}$) (G) Gal8-SLAP$_{TAG}$ (H) GST-SLAP$_{TAG}$. MK = protein marker (kDa); IN = input; FT = flowthrough; W =
542 wash; E = elution.

543 **Figure 6: Western blot analysis of purification of SLAP-tagged proteins using different expression systems.**
544 (A) Purification of SLAP$_{ASE}$ (human rhinovirus 3c fused to SLAP$_{TAG}$) protease expressed in *Pichia pastoris*. (B)
545 Purification of SARS CoV2 Spike-SLAP$_{TAG}$ protein expressed in HEK293 cells. MK = protein marker (kDa); IN =
546 input; FT = flowthrough; W = wash; E = elution.

547 **Figure 7: Analysis of Bio-Matrix stability in time and reuse.** (A) The figure compares (H_6)-GFP-SLAP$_{TAG}$
548 purification yield of SLAP$_{TAG}$-based affinity chromatography at different times when it is conserved at -20ºC.
549 (B) Figure compares (H_6)-GFP-SLAP$_{TAG}$ purification yield of SLAP$_{TAG}$-based affinity chromatography for
550 different cycles of reuse. The asterisk denotes a significant difference using the ANOVA method, Bonferroni
551 test (** $p = 0,0059$; *** $p = 0,0002$; **** $p < 0.0001$)

552

553 **Figure 8: SLAP$_{TAG}$ removal.** (A) Graphical description of the protocol to remove the SLAP$_{TAG}$ using SLAP$_{TAG}$-
554 based affinity chromatography. SDS-PAGE of purification fractions of SLAP$_{TAG}$ removal protocol stained with

555 Coomassie blue solution (B) or under UV light (C). Western Blot of purification fractions of $SLAP_{TAG}$ removal
556 protocol revealed with anti-SLAPTAG (D) or anti-GFP (E) antibodies. $SLAP_{ASE}$ = purified protease; IN = input;
557 FT = flowthrough; E = elution; MK = protein marker (KDa)

558

559 **Figure 9: GFP-$SLAP_{TAG}$ purification using Magnetic Bio-Matrix.** (A) Graphical description of the purification
560 protocol for magnetic Bio-Matrix. (B) Photo of 1,5 tubes ml containing fractions of GFP-$SLAP_{TAG}$ magnetic
561 purification under UV light. (BM_{mag} = magnetic Bio-Matrix; IN = input; FT = flowthrough; W = wash; E =
562 elution. (C) Tubes containing magnetic purification fractions are seen under UV light. GFP input
563 fluorescence is recovered in the eluate.

564 **Table S1**: Purification table of GFP-$SLAP_{TAG}$ using the Biomatrix
565

566 **Supplementary Video 1:** Magnetic affinity chromatography using BIOMATRIX

567

568 **TABLE 1**: Bacterial strains and plasmids used in this study

Strain		
E. coli DH5α	F−ϕ80*lac*ZΔM15 Δ(*lac*ZYA-*arg*F) U169 *rec*A1 *end*A1 *hsd*R17(rK−, mK+) *pho*A *sup*E44λ- *thi*-1 *gyr*A96 *rel*A1	Invitrogen
E. coli BL21 Codon plus	[*omp*T *hsd*S(rB– mB–) *dcm* + Tcr *gal* λ (DE3) *end*A Hte Cmr]	Stratagen
B. subtilis	Wild type strain var. *natto*	ATCC 15245
Pichia pastoris	*P. pastoris* strain GS115	BioRad, USA
Plasmid		
pET28-eGFP-SlpA	A vector containing the GFP gene from *Aequorea victoria* fused to $SLAP_{TAG}$	[18]
pET22-eGFP-SlpA	A vector containing the GFP gene from *Aequorea victoria* fused to LEVLFQGP sequence and $SLAP_{TAG}$	This study
pGEX-SlpA	A vector containing GST form *Shitosoma japonicum* fused to $SLAP_{TAG}$	[12]
pLC3-EITH7-SlpA	A vector containing EspA-Intimin-Tir fused genes from STEC *E. coli* fused to $SLAP_{TAG}$	[12]
pLC3-Omp19-SlpA	A vector containing the Omp19 gene from *Brucella abortus* fused to $SLAP_{TAG}$	[12]
pLC3-FliC-SlpA	A vector containing the FliC gene from *Salmonella enterica* fused to $SLAP_{TAG}$	[12]
pLC3-Gal8-SlpA	A vector containing the Gal8 gene from *Mus musculus* fused to $SLAP_{TAG}$	[12]
pET28-Lys-SlpA	A vector containing the Lysozyme gene from *Gallus* fused to $SLAP_{TAG}$	This study
pMAL-c5X-HRV3c-SlpA	A vector containing human rhinovirus (HRV) type 14 3C protease gene fused to $SLAP_{TAG}$ (SLAPase)	This study
pGEX-2T-EspA-SlpA	A vector containing the EspA gene from STEC *E. coli* fused to $SLAP_{TAG}$	This study
pPICZalphaB-HRV3c-SlpA	A vector containing human rhinovirus (HRV) type 14 3C protease gene fused to $SLAP_{TAG}$ (SLAPase)	This study
Addgene #154754	A vector containing the sequence of SARS CoV2 Spike ectodomain Hexa-pro	[29]
pSpike-$SLAP_{TAG}$	Plasmid Addgene #154754 fused with the $SLAP_{TAG}$	This study
pLysS	Vector for expression of T7 lysozyme.	Novagene

569